Plasma Sources Sci. Technol. 3 (1994) 575–583. Printed in the UK

Effect of the waveform of voltage pulses on the efficiency of ozone synthesis in corona discharges

E A Gordeyenya and A A Matveyev

High-Voltage Research Centre of the All-Russian Electrotechnical Institute, 143500, Istra-2, Zavodskaya st, Moscow region, Russia

Received 1 October 1993; in final form 24 February 1994

Abstract. The efficiency of ozone synthesis in pulsed corona discharge has been investigated for a system consisting of a plane electrode and a wire. The corona was sustained by positive and negative aperiodical pulses of microsecond and sub-microsecond duration as well as by alternating-sign pulses of microsecond duration of oscillation frequency 1.5–3.1 MHz. In a number of experiments, a fibre glass dielectric barrier was placed on the earthed plane. In the case in which the streamer crossed the discharge gap, employment of the dielectric barrier allowed us to estimate the relative contribution of the primary streamer to the overall production of ozone. It is shown that a combination of an alternating-sign pulse and a dielectric barrier permits one to obtain simultaneously the greatest ozone yield in a single pulse and the best plasma-chemical efficiency of ozone synthesis.

1. Introduction

Excitation of a corona discharge represents a relatively simple way of producing weakly ionized ($n_e/n_m = 10^{-4}$–10^{-5}, where n_e is the density of electrons and n_m is the density of heavy particles) low-temperature non-equilibrium plasmas in a wide range of gas pressures and temperatures. One of the properties of the corona discharge that is of interest for applications is its ability to produce considerable amounts of chemically active particles (radicals), thereby initiating gas-phase chemical reactions, whose performance under conditions of thermodynamic equilibrium would require temperatures of several thousands of kelvins. When the initial gas mixture contains oxygen and water vapour the intermediate reaction products include such powerful oxidizers as O, OH, HO_2, H_2O_2 and O_3, with the absence of strong heating of heavy particles in the corona discharge being favourable for preservation of relatively fragile ozone molecules.

The aforesaid has given rise to interest in the corona discharge as a way of increasing the degree of oxidation of the lowest nitrogen and sulphur oxides in flue gases for the purpose of more effective removal of NO_x and SO_x as well as to produce ozone from air or oxygen, which is attractive because of its simplicity and insensitivity to the presence of dust in the air.

Since electron-induced plasma-chemical processes proceeding in the discharge are sensitive to the electric field strength (which determines the electron energy distribution function and so influences the energy-loss spectrum in the plasma), changing the geometry of the discharge gap, feeding conditions and rate of gas flow allows one to affect selectively specified reactions in the discharge plasma. In particular, in production of ozone from air, this property of the corona discharge allows one to reduce significantly the relative yield of nitrogen oxides [1].

As is shown in [2], in producing ozone from air, the best plasma-chemical efficiency of ozone synthesis, with the discharge fed by constant voltage, is observed in streamer regimes. In this case the efficiency of ozone synthesis may reach 20–30 g kW^{-1} h^{-1} for dried air [2] and 90 g kW^{-1} h^{-1} for O_2 [3].

Further increase in efficiency of ozone production in the corona discharge is connected with application of a pulsed voltage. Employment of short (tens or hundreds of nanoseconds) rapidly rising ($dU/dt > 10^{12}$ V s^{-1}) voltage pulses, changing the dynamics of volume charge formation in the gap, allows one to increase values of parameters E/n_m and n_e at the front of the streamer [4] and thereby to increase the path length of streamers [5]. When employing such corona feeding regimes, ozone yields may be as high as 100 g kW^{-1} h^{-1} of deposited energy or may even exceed this value [6–8].

Substantiation of regimes of corona pulse feeding with respect to increasing the efficiency of ozone synthesis adduced in [7, 9] allows one to consider sub-microsecond pulses as preferable owing to lower energy losses on gas heating and lower ozone destruction, though pulses with $\tau = 10\ \mu s$ (half-height) applied in [8] provided ozone yields of 110–145 g kW^{-1} h^{-1}, that is, not less than in [7], where pulses with $\tau = 100$–200 ns and values of dU/dt close to those in [8] were used. However, it should be noted that the correctness of

0963-0252/94/040575 + 09$19.50

determining the energy deposited in [8] is in doubt. Indeed, the discharge current used in [8] for calculation of the energy deposited, I_{dis}, was determined as the difference between total measured current, I_m, and the induced capacitive component, I_{ind}. The value of I_{ind} was determined in a separate experiment in which the streamer zone of the discharge was replaced by a cylindrical electrode selected so that, when a high-voltage pulse was applied, almost no discharge could be observed. Such a replacement does not allow one to take into account changes in dynamic capacitance of the streamer zone during its development. The current I_{dis} obtained in such a manner had a triangular shape, of half-height duration about 50 ns, and contained significant noise. In view of the aforesaid, the values of the energy deposited calculated in [8] seem to be underestimated.

The specific energy expenditures for ozone production calculated from the total energy $CU^2/2$ of the feeding capacitor (ξ_c) as well as from the energy deposited in the discharge (ξ_0) vary within wide limits, depending on feeding pulse parameters and discharge gap geometry. As this takes place, the values of ξ_c and ξ_0 may differ by orders of magnitude [6], so that regimes of corona feeding attractive with respect to ξ_0 may turn out to be absolutely unacceptable with respect to ξ_c. It is obvious that, in order to choose the regime of corona feeding in the ozonator device, one should know the dependences of ξ_c and ξ_0 on the feeding pulse characteristics for a given geometry of discharge gap. Owing to the lack of detailed literature data of this kind, in particular for the wire–plane system, the authors undertook the present study of the dependences of ξ_c and ξ_0 on the duration of the aperiodical feeding pulse of positive and negative polarity (PP and NP) and the electrode gap d, with and without a dielectric barrier on the earthed plane.

It is known [10] that, with corona discharges fed by alternating-sign pulses, employment of a dielectric barrier allows one to increase the ozone yield and to reduce ξ_0. Continuing the investigations started in [10], the authors also present the results of experimental studies of ozone production efficiency in the corona discharge in undried atmospheric air fed by alternating-sign pulses from three different power sources. For all types of pulsed power sources the validity of introducing a dielectric barrier with regard to reduction in ξ_c is shown.

2. Experimental set-up

A schematic sketch of the experimental set-up is presented in figure 1. Experiments were performed with a wire–plane electrode system. The high-voltage electrode (nichrome wire 0.2 mm in diameter wound on a dielectric frame of size 360 mm × 300 mm with a pitch of 20 mm) was placed in a reaction chamber of internal size 310 mm × 412 mm × 76.5 mm (volume 100 l) fabricated from organic glass and fitted with quartz windows for

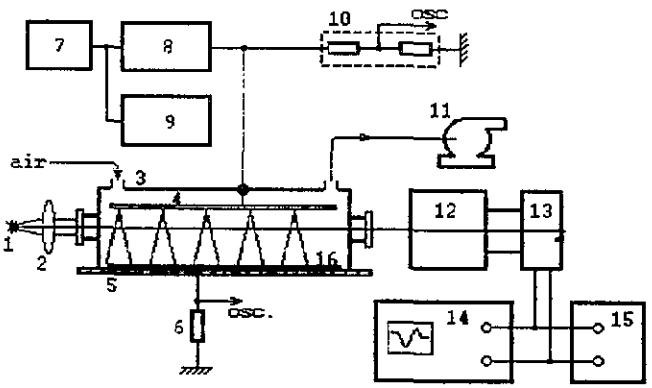

Figure 1. Schematic sketch of the experimental set-up: 1, Hg arc lamp; 2, collimator; 3, reaction chamber; 4, high-voltage electrode; 5, earthed plane; 6, shunt; 7, master oscillator; 8, high-voltage aperiodical pulse shaper; 9, high-voltage alternating-sign pulse shaper; 10, voltage divider; 11, backing pump; 12, monochromator; 13, photomultiplier; 14, oscillograph; 15, digital voltmeter; and 16, dielectric barrier.

passage of diagnostic UV radiation from a mercury lamp. The plane electrode made of Al alloy was earthed through a low-inductive resistance, $r = 2.002\,\Omega$. Discharge voltage was measured by an ohmic divider. As a source of high-voltage aperiodical pulses, an RC circuit commutated by a controlled spark gap was used. The feeding condenser of 1.33 nF capacitance was charged to 55 kV, with discharge time constant, when running idle, variable in the range 0.13–45 μs by means of a set of resistors.

Spiral generators (strip lines rolled up in a spiral) of oscillation frequencies 2.6 and 3.1 MHz and a pulse transformer with a ceramic capacitor ($C = 20$ nF) in primary winding circuit and oscillation frequency of 1.51 MHz were used as a source of alternating-sign pulses. When running idle, all sources indicated developed a voltage above 150 kV, with charging voltages of 5, 9 and 10 kV, respectively.

In the course of experiments the discharge voltage and the current through the earthed electrode were registered by a HV oscillograph of bandwidth 50 MHz, allowing us to calculate the energy absorbed in the discharge. Ozone concentration in the reaction chamber was determined by absorption of UV radiation at $\lambda = 2537$ Å about 30 s after the end of the package of high-voltage pulses, when the relative absorption became settled. The values of $[O_3]$ plotted on graphs and used in calculations of specific energy expenditures were obtained by averaging over ten measurements executed under the same conditions. For each series of measurements, the value of the root mean square deviation was calculated, which turned out to amount to about 2%. Experiments were performed in atmospheric undried air without pumping; the number of high-voltage pulses in a package was varied from 200 to 500 at pulse rate 50 pulses per second. In a number of experiments the earthed plane was covered by a fibre glass dielectric barrier 410 mm × 310 mm of thickness 2.5 mm.

3. Results and discussion

3.1. Aperiodical pulses

3.1.1. Positive polarity. Oscillograms of discharge voltage and current as well as the dynamics of energy absorption in the discharge are presented in figure 2. As may be seen therein, the presence of the dielectric barrier does not affect the time-dependence of the discharge current until time τ_4. Two maxima are clearly distinguishable on the current oscillogram, that of duration $\tau_1 = 25$ ns being conditioned by charging of the inter-electrode capacitance, C_{wp}. After completion of charging, a fast rise of the current is observed in time $\tau_6 = 20$–25 ns until the value I_2, following which the rate of current rise dI/dt decreases drastically; the current reaches its maximum value I_3 and falls to $0.1I_3$ in about 400 ns. The duration of the second pulse measured at the half-height, τ_2, varies from 100 to 200 ns according to the gap separation, d. It should be noted that, when photographing from the oscillograph screen, 15–20 oscillograms coincided in all cases within the thickness of the beam (about 1 mm) at scanning rate 100 ns cm^{-1}. This indicates the temporal stability of the corona discharge development, with the scatter of lag time between the moment of energizing the discharge gap and the beginning of current rise being below 10 ns. Temporal characteristics of the second pulse of current, τ_2 and τ_6, match those of the streamer process [11].

Everywhere over the range of d realized in the experiment, the corona discharge exhibits channel structure, with the luminosity of channels increasing as d is reduced and decreasing drastically upon introduction of the dielectric barrier into the discharge gap.

The divergence of current oscillograms at $t = \tau_4$ connected with introduction of the barrier into the gap is evidently a consequence of the barrier charging and is possible only after the streamer has reached the barrier. This allows one to distinguish two temporal areas on the oscillograms: before and after streamers have crossed the gap. On the other hand, the coincidence of current oscillograms with and without the barrier indicates that the streamer does not reach the earthed electrode.

Figure 3 displays the dependence of ozone yield N in a single pulse on the electrode separation d for various values of time constant RC of aperiodical pulse shaping. The maximum yield of ozone is observed in the absence of the dielectric barrier at $d = 25$ mm for all values of RC.

With the dielectric barrier, the dependence $N(d)$ has a more intricate character, the main differences being that the maximum ozone yield is observed at $d = 30$ mm, the region of N falling off at $d < 30$ mm is absent (as is the bright luminosity of channels); ozone yield with the barrier is less than half that without the barrier, all other things being the same.

The dependence of ozone yield on the number of wire turns on the frame for the PP, $RC = 5$ μs, $d = 25$ mm, is weak with and without the barrier as shown in figure 4. Some gain in ozone yield may be obtained by increasing the diameter of the corona wire to 0.4 mm.

The dependence of the energy W deposited in the discharge on d (figure 5) is monotonic with and without the barrier. Introduction of the barrier lowered the energy deposited, on average, by 20% in the case that the streamer reached the earthed electrode. At $RC = 5$ μs and in the absence of the barrier up to 66% of the energy stored in the power supply was absorbed in the gas.

Specific energy expenditures $\xi_0(d)$ calculated from

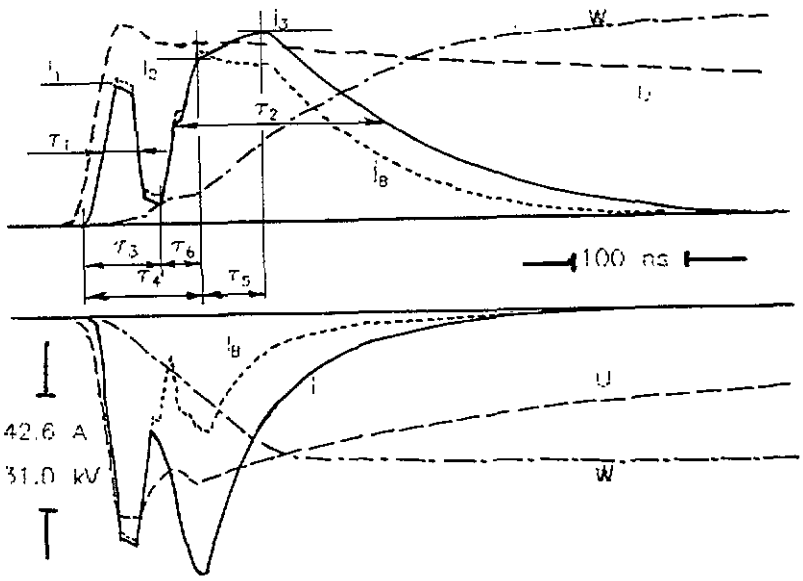

Figure 2. Oscillograms of voltage and current, $U(t)$, $I(t)$ and the energy absorbed in the discharge, $W(t)$. (*a*) Positive pulses, $d = 50$ mm, $RC = 5$ μs; (*b*) negative pulses, $d = 22.5$ mm, $RC = 0.58$ μs. I_B corresponds to the current in the presence of the barrier.

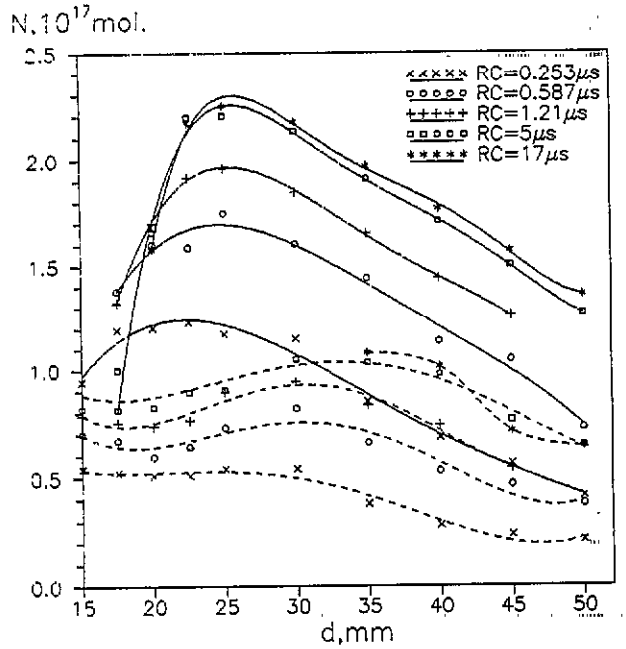

Figure 3. Ozone yield in a single pulse for positive polarity with and without the dielectric barrier (broken and full curves, respectively).

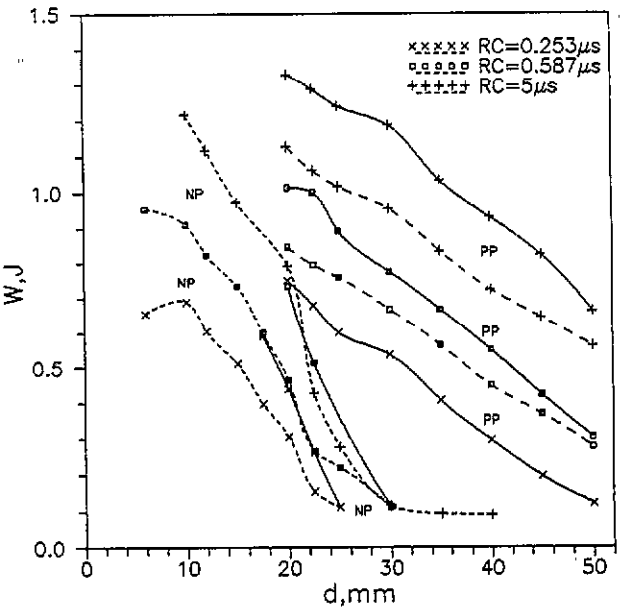

Figure 5. Energy absorbed in the discharge versus d (aperiodical pulses). Broken curves correspond to the case with the dielectric barrier.

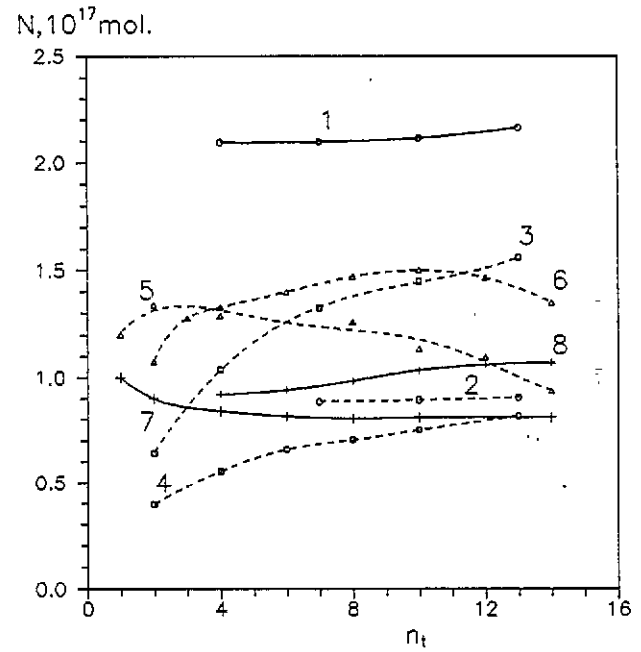

Figure 4. Ozone yield N as a function of the number of wire turns. Aperiodical pulses: 1 and 2, positive polarity, $d = 25$ mm, $RC = 5$ μs; 3, negative polarity, $d = 10$ mm, $C = 1.33$ nF, $RC = 1.21$ μs; and 4, negative polarity, $d = 10$ mm, $C = 0.453$ nF, $RC = 1.75$ μs. Alternating-sign pulses ($f = 3.1$ MHz): positive (6 and 8) and negative (5 and 7) polarity of the first half-wave; $d = 27.5$ mm (5 and 6) and 35 mm (7 and 8). Broken curves correspond to the case with the dielectric barrier.

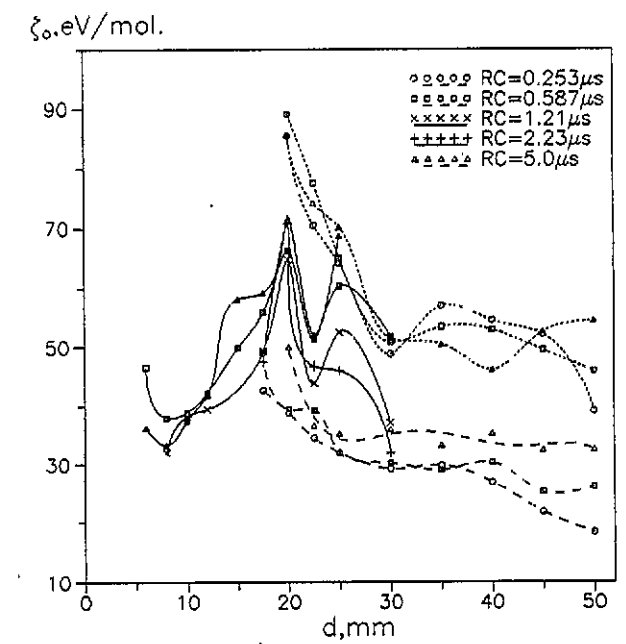

Figure 6. Specific energy expenditures for ozone synthesis versus d (aperiodical pulses). Full curves are for negative pulses with the barrier; broken curves are for positive pulses without the barrier; and dotted curves are for positive pulses with the barrier.

$N(d)$ and $W(d)$ are presented in figure 6. In the absence of the barrier the dependence $\xi_0(d)$ is monotonic; in the region $d < d(N_{max})$ (here $d(N_{max})$ is the value of d corresponding to the maximum ozone yield) ξ_0 rises sharply as the d decreases, whereas at $d > d(N_{max})$ only a slight fall is observed, which is more pronounced for lesser values of the feeding pulse duration. With the dielectric barrier, energy expenditures are twice as much; the dependence $\xi_0(d)$ in greater detail is discussed below.

3.1.2. Negative polarity. Voltage and current oscillograms and the dependence $W(t)$ are shown in figure 2. Unlike the PP, in this case the dielectric barrier restricts

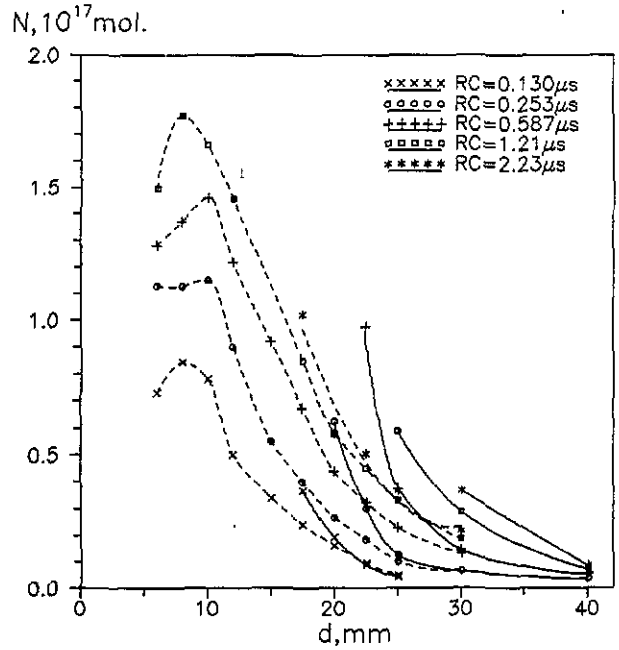

Figure 7. Ozone yield in a single pulse for negative polarity with and without the dielectric barrier (broken and full curves, respectively).

the charge transferred in a pulse and the energy deposited in the gas to a greater extent. Besides, at $d > 30$ mm only the first current jump connected with charging of the inter-electrode capacitance is observed, and hence current oscillograms with and without the barrier coincide. The duration of the second current pulse does not exceed 100 ns in all cases.

The dependence $N(d)$ (figure 7) indicates that maximum ozone yield was obtained at $RC = 0.58$ μs and was significantly lower than at the PP. Employment of the dielectric barrier allows one to increase N essentially by increasing pulse duration and decreasing d without spark-over of the discharge gap. At the PP the maximum ozone yield was obtained in the absence of the barrier, as opposed to the NP case.

The dependences $W(d)$ and $\xi_0(d)$ are presented in figures 5 and 6. It should be noted that, at the NP, the dependence $\xi_0(d)$ has an intricate non-monotonic character, with the peculiarities of its behaviour increasing as the feeding pulse duration is reduced. The lowest level of specific energy expenditure realized at the NP amounts to about 32 eV mol^{-1}, which is almost twice as much as at the PP (18 eV mol^{-1}).

At the NP, varying the length of the corona wire essentially affects ozone yield (figure 4). In this case, with the dielectric barrier, the energy stored in the power supply, $CU^2/2 = 2.01$ J, evidently permits one to obtain greater quantities of O_3 with the number of turns $n_t > 13$, which, however, would require increasing the dimensions of the reaction chamber. A similar situation arises with the stored energy decreased by a factor of three, so the value of specific energy expenditure for the NP with the barrier, $\xi_c = 29$ W h g^{-1}, is only tentative. In the absence of the dielectric barrier, the dependence of N on the number of turns has a maximum at $n_t = 8$; in this case ξ_c is more than that with the barrier by a factor of 2.5.

3.1.3. Discussion. According to the concepts elaborated in [2, 12, 13], streamer development from the positive point proceeds in three steps: (i) propagation of the primary streamer; (ii) a resistive stage in which the secondary luminous wave arises and the current decays; and (iii) spark transition. Regimes of corona discharge feeding accompanied by initiation of breakdown are evidently unacceptable for the purpose of ozone synthesis and are not discussed in the present paper.

As a characteristic of conditions in the discharge gap during the second 'resistive' stage, the mean value of the parameter E/n_m, $\kappa_m = U/(dn_m)$, may be used with due caution, which determines the balance of concentrations of charged particles and conditions of plasma-chemical reactions proceeding with their participation.

At the beginning of the decay portion of current oscillograms, the value of κ_m varied under our conditions within the limits 35–70 Td, depending on d, and, on completion of the current in the gap, it was established at a value 28–33 Td, which was always less than the static breakdown one.

As in [14], current decay has an exponential character conditioned by electron attachment to oxygen molecules. The dependence of the decay time constant τ_{att} on d is displayed in figure 8 as well as the calculated dependence of τ_{att} on the parameter E/n_m, accounting for the processes of three-particle and dissociative attachment and obtained from a numeric solution of the kinetic Boltzmann equation for electrons. From figure 8, it follows that the value $\tau_{att} = 80$ ns corresponds to

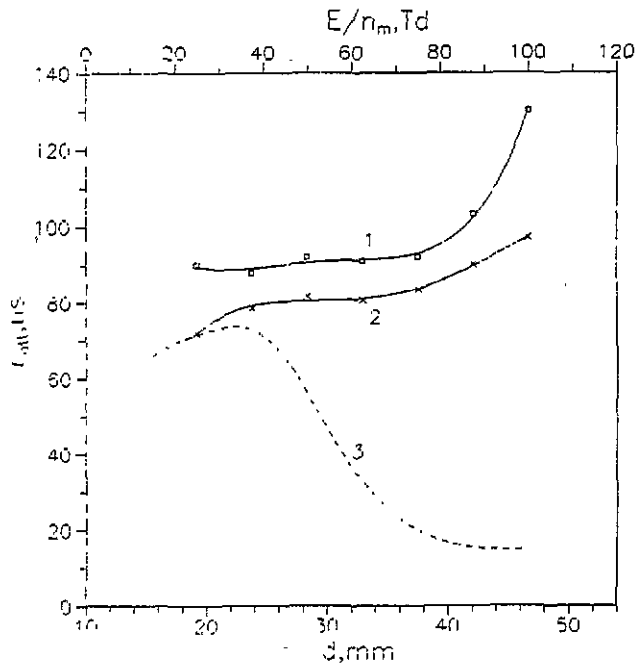

Figure 8. Experimental time constant of current decay, $\tau_{att}(d)$ (positive pulses; $RC = 5$ μs; curve 1, without the barrier, curve 2, with the barrier), and theoretical time constant of electron attachment, $\tau_{att}(E/n_m)$ (curve 3).

$E/n_m \simeq 35$ Td, which agrees satisfactorily with experimental results. However, this model cannot provide an explanation for the rise in τ_{att} occurring with increasing d. Such a discrepancy may be connected with electron detachment from negative ions O_2^- in collisions with metastable oxygen $O_2(^1\Delta_g)$ [15].

As mentioned above, at the NP and for $d > 25$ mm, $RC < 5$ μs, only the first current peak connected with electrode capacitance charging was observed (at $RC > 5$ μs, breakdown occurred at any value of d). The value of discharge gap capacitance measured at low voltage is approximately 1.5 times smaller than the value obtained from the oscillograms of voltage and current. Besides, at $d > 25$ mm the energy deposited in the discharge is independent of d. Presented data testify that streamers do not develop at the NP for $d > 25$ mm, though there is an ionized region near the wire. At the PP, a similar situation was not observed under any conditions.

In an effort to determine the relative contributions of distinct stages of streamer process development to the overall ozone yield, it is necessary to analyse conditions existing in the discharge gap at every stage.

According to theoretical calculations [16] and results of spectroscopic measurements [17, 18] the electric field at the head of a propagating streamer amounts to 200–300 Td. From the analysis [19] of the distribution of the energy gained by electrons in the applied electric field over the degrees of freedom of the N_2 and O_2 molecules, the indicated values of the parameter E/n_m are optimal for excitation of processes leading to O_2 dissociation, namely direct dissociation by electron impact and excitation of electronic levels of N_2 [20]. However, on account of the small size of the streamer head (tens of micrometres) and high speed of its propagation (about 10^8 cm s^{-1}), the duration of action of the streamer head field in a fixed spatial point is very short (a fraction of a nanosecond). Conditions in the streamer channel depend essentially on whether the streamer reaches the opposite electrode. In the case in which streamer propagation is limited to only a part of the discharge gap, the field in the streamer channel is maintained at 5–7 kV cm^{-1} [5, 18], which corresponds to effective excitation of the vibrational levels of N_2 molecules, with O_2 dissociation being insignificant [19]. This field is maintained during a period longer than the life time of electrons determined by attachment to O_2 molecules. Under similar conditions only a small percentage of the energy stored in the power source is deposited in the gas [6, 7].

When the streamer crosses the discharge gap and the secondary luminous wave arises, results of spectroscopic measurements [21] allow one to suggest existence of near-breakdown fields in a sizable part of the gap adjacent to the wire. The duration of action of these fields is of order tens of nanoseconds and permits one to expect a considerable yield of ozone at this stage.

In this connection it is of interest to calculate separately the absolute and relative energy deposited in the gas at the first stage of the streamer process (W_w and W_w/W; figure 9) and to correlate them with the experimental dependences of ozone yield per pulse and specific energy expenditures (figures 3 and 6).

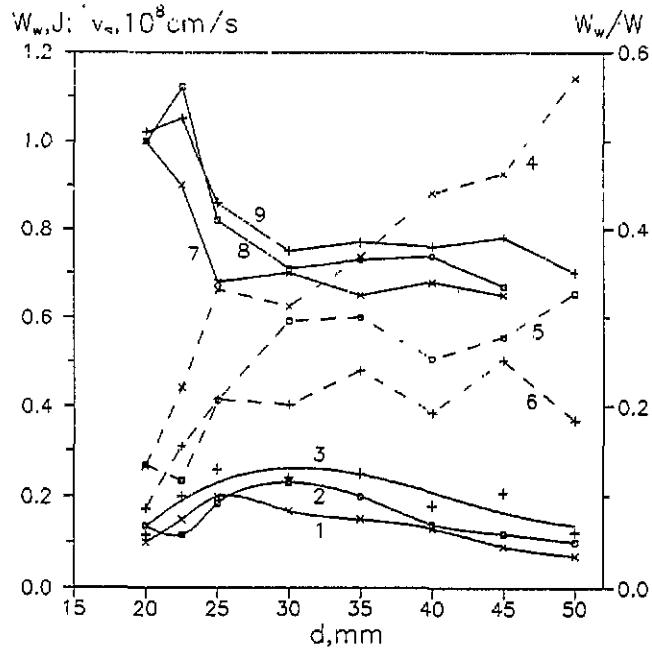

Figure 9. Absolute (1–3) and relative (4–6) energy deposited in the discharge during the primary streamer stage and mean values of streamer propagation velocity (7–9). Positive polarity; $RC = 0.253$ μs (1, 4 and 7), 0.587 μs (2, 5 and 8) and 5 μs (3, 6 and 9).

Figures 3, 6 and 9 indicate correlations between the dependences $W_w(d)$ and $N(d)$ as well as between $W_w/W(d)$ and $\xi_0(d)$. An analysis of the correlating functions allows one to suggest, in particular, that the main reason for ozone yield decreasing at $d < 25$ mm is reduction in W_w due to rising streamer velocity (figure 9).

An increase in ozone synthesis efficiency with increasing share of W_w in the overall energy deposited shows that conditions during the first stage of the streamer process are more favourable to O_3 generation. However, experiments with the dielectric barrier demonstrate that the second stage accounts for up to half the ozone formed during a pulse and the greater part of energy absorbed in the gas.

Thus, in deciding on parameters of the aperiodical feeding pulse, it is necessary to take into account that production of the maximum amount of O_3 in a corona discharge for a given energy stored in the power supply requires observance of the following rules.

(i) The primary streamer should cross the discharge gap.

(ii) The amount of energy deposited in the gas at the primary streamer development stage should be the greatest, which corresponds to the optimal value of d.

(iii) The duration of the feeding pulse should be as long as possible but excluding occurrence of breakdown; in so doing, it should be noted that, at $RC > 5$ μs, the dependence $N(RC)$ is weak (figure 10).

However, in this case the efficiency of ozone syn-

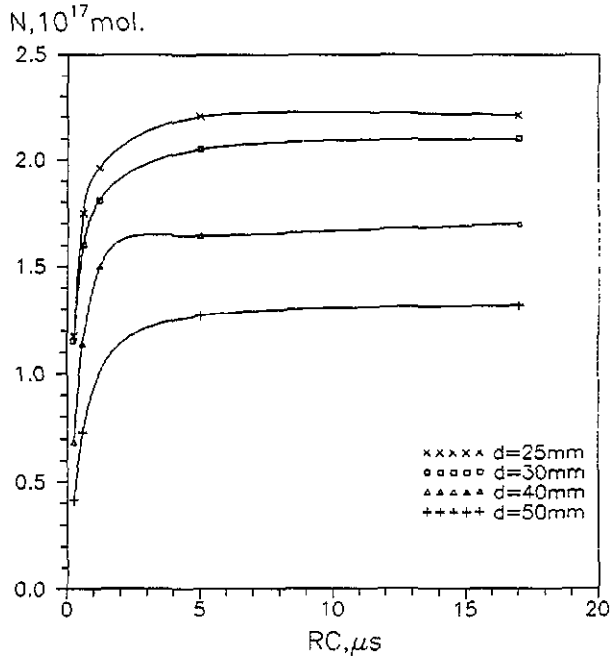

Figure 10. Ozone yield as a function of *RC* (aperiodical pulses, positive polarity).

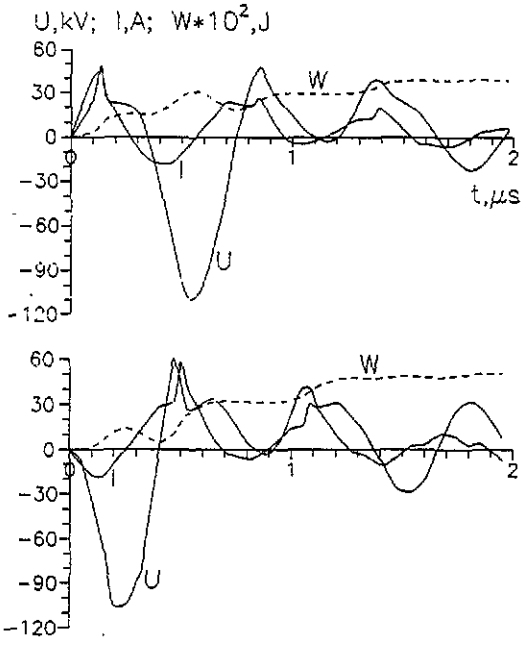

Figure 11. Oscillograms of voltage and current, $U(t)$, $I(t)$, and energy absorbed in the discharge, $W(t)$ for alternating-sign pulses ($f = 1.5$ MHz) with the barrier absent and $d = 40$ mm.

thesis is essentially lower than the best value achieved experimentally. On the other hand, for regimes with optimum plasma-chemical efficiency of O_3 generation, the coefficient of energy utilization is small and, consequently, ozone yield is low. A different situation arises with the use of alternating-sign pulsed feeding.

3.2. Alternating-sign pulses

As shown in [10], employment of alternating-sign pulse voltages for corona discharge feeding allows one to achieve relatively high efficiency ozone synthesis in air and oxygen, provided that a dielectric barrier is used on the earthed plane electrode. In this case conditions of barrier operation are essentially easier than in a barrier discharge.

Typical oscillograms of voltage and current for the power supply using a pulse transformer, at the PP and NP of the first half-wave, are shown in figure 11, as are the temporal changes in energy absorbed in the discharge. Streamer peaks accompanied by stepwise increase in deposited energy are clearly distinguishable on the oscillograms. During the first half-wave at the NP, streamer peaks are not observed and the energy absorption is small, though the voltage across the gap exceeds 100 kV (at $d = 40$ mm). At $d < 30$ mm streamers arise even during the first negative half-wave, in which case the energy returned from the discharge gap to the power supply becomes low. Introduction of a dielectric barrier into the gap slightly decreases the amplitude of streamer current peaks and increases the remaining voltage. Hence the energy deposited in the gas rises.

The dependences of O_3 yield on d for three different sources of alternating-sign pulse voltage at the PP and NP of the first half-wave are plotted in figure 12. As for the aperiodical pulse, introduction of the dielectric barrier allows one to increase O_3 yield within a certain range of d. At the PP of the first half-wave, the greatest yield was observed at similar values of d for all used sources of alternating-sign pulses. At the NP, the maximum N for spiral generators is less than at the PP due to the fact that the amplitude of the second half-wave is about 1.5 times that of the first half-wave. The effect of the polarity of the first half-wave for the pulse transformer is small because of lower differences in voltage amplitudes between first and second half-waves when running idle. Optimization of corona wire length for the power source of frequency 3.1 MHz permitted us to increase ozone yield (figure 4); in this case $\xi_c = 22.5\ \mathrm{W\,h\,g^{-1}}$. Note that, in ozonizers based on barrier discharge, the value ξ_c (including air conditioning and cooling) amounts to 20–30 $\mathrm{W\,h\,g^{-1}}$, depending on productivity of the ozonizer.

The values of the energy deposited in the discharge and the specific energy expenditures for the source with the pulse transformer (figure 13) calculated from the oscillograms show a rather high efficiency of O_3 generation ($\xi_0 = 10\ \mathrm{W\,h\,g^{-1}}$). Thus the greatest ozone yield *and best plasma-chemical efficiency are achieved under* the same conditions, which is a significant advantage over corona feeding by aperiodical pulses. Ozone yield normalized to the energy stored in the power source amounts to $37.7\ \mathrm{g\,kW^{-1}\,h^{-1}}$ in this case. The results presented are not the best ones for the power source involved, because the diameter and length of the corona wire were not optimal.

The efficiency of corona feeding by alternating-sign pulses of oscillator frequency of the order of several megahertz appears to be connected with the possibility

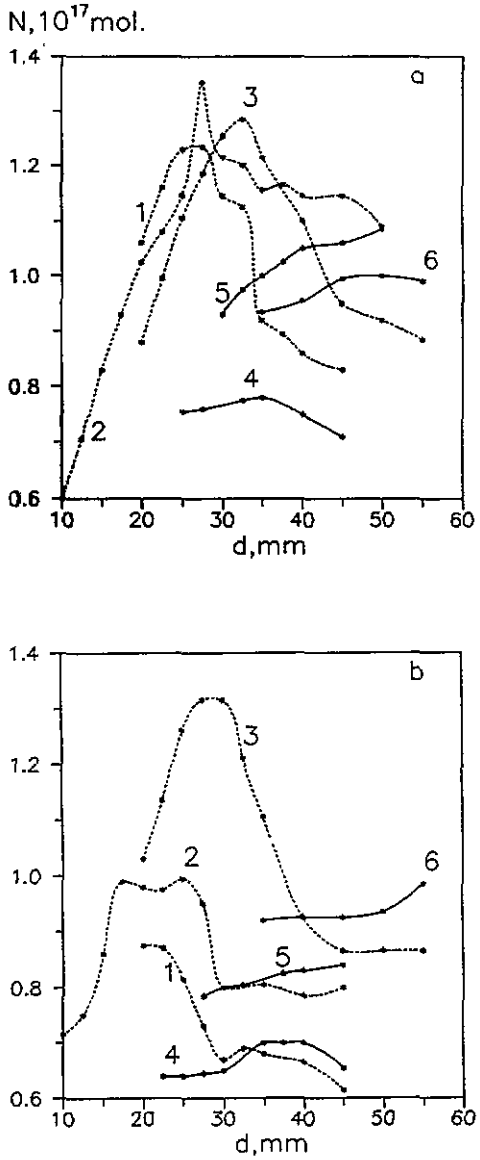

Figure 12. Dependence of ozone yield in a single pulse on d. Power source: 1 and 4, spiral generator, $f = 2.6$ MHz; 2 and 5, spiral generator, $f = 3.1$ MHz; 3 and 6, pulse transformer, $f = 1.5$ MHz. Polarity of the first half-wave: (*a*) positive, (*b*) negative. Broken curves correspond to the case with the dielectric barrier.

of exciting several streamers during a single pulse in a time shorter than the characteristic time of ozone formation in a three-particle reaction.

It is known that ignition of corona discharge in flue gases by use of short rapidly rising pulses allows efficient removal of the lowest oxides of nitrogen and sulphur, which are responsible for acid rain [9]. Among the particles forming in plasma, radicals OH, H, O and HO_2 are of greatest importance in the NO_x and SO_x removal processes [22]. As theoretical calculations [16] of streamer propagation in flue gases show, the ratio between yields of O and OH radicals depends only slightly on feeding conditions. Thus, it may be expected that regimes of corona discharge feeding by alternating-sign pulse voltage ensuring effective generation of O_3 can be effective with respect to electrochemical treatment of flue gases.

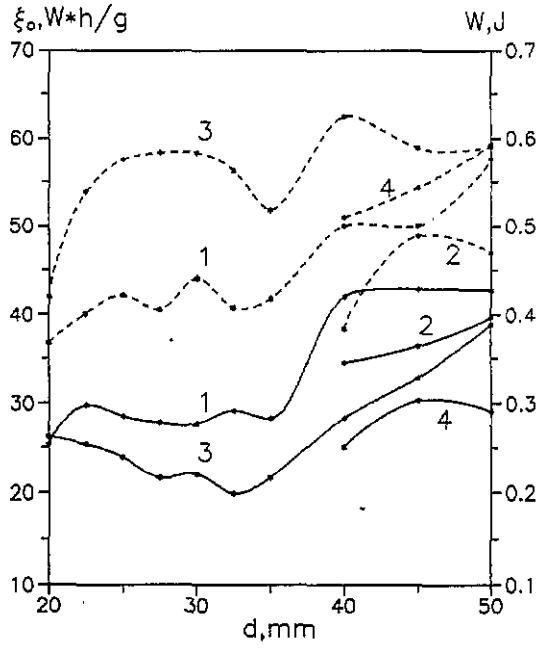

Figure 13. Dependences $\xi_0(d)$ (full curves) and $W(d)$ (broken curves) for alternating-sign pulses, $f = 1.5$ MHz. Polarity of the first half-wave: 1 and 2, positive; 3 and 4, negative. 1 and 3 are with the barrier; 2 and 4 are without the barrier.

References

[1] Peyrous R and Lapeyre R-M 1982 *Atmospheric Environment* **16** 959–68.
[2] Lecuiller M and Goldman M 1988 *J. Phys. D: Appl. Phys.* **21** 51–6
[3] Peyrous R and Lacaze C 1986 *Ozone Sci. Eng.* **8** 107–28
[4] Creyghton Y, van Veldhuizen E M and Rutgers W R 1992 *NATO Advanced Research Workshop on Non-Thermal Plasma Techniques or Pollution Control, Cambridge University, September 21–25*
[5] Gallimberti I 1979 *J. Physique* C7 193–250
[6] Amirov R H, Asinovsky E I, Samoilov I S and Shepelin A V 1992 *Khim. Vysokih Energiy* **26** 76–81 (in Russian)
[7] Masuda S, Sato M and Seki T 1986 *IEEE Trans. Ind. Appl.* **22** 886–91
[8] Mizuno A and Kamase Y 1987 *Conf. Record IEEE Industrial Application Society—22nd Annual Meeting, Atlanta, Georgia, October 18–23* part 2, pp 1534–8
[9] Masuda S 1988 *Pure Appl. Chem.* **60** 727–31
[10] Gordeyenya E, Kostinsky A, Trapeznikov A and Terechin V 1991 *Proc. XX ICPIG, Barga, Italy, July 8–12* pp 923–4
[11] Giao T N and Jordan J B 1968 *IEEE Trans. Power Appar. Syst.* **87** 1207–15
[12] Marode E 1975 *J. Appl. Phys.* **46** 2005–15
[13] Bastien F and Marode E 1985 *J. Phys. D: Appl. Phys.* **18** 377–93
[14] Sigmond R S and Goldman M 1982 *Gaseous Dielectrics: Proc. 3rd Int. Symp., Knoxville, Tennessee, March 7–11* vol 3, pp 53–9
[15] Lowke J J 1992 *J. Phys. D: Appl. Phys.* **25** 202–10
[16] Gallimberti I 1988 *Pure Appl. Chem.* **60** 663–74
[17] Kondo K and Ikuta N 1980 *Proc. VI Int. Conf. Gas Discharges and their Applications, Edinburgh* pp 118–21

[18] Gallimberti I, Hepworth J K and Klewe R C 1974 *J. Phys. D: Appl. Phys.* 7 880–98
[19] Aleksandrov N L, Vysikailo F I, Islamov R Sh, Kochetov I V, Napartovich A P and Pevgov V G 1981 *Teplofiz. Vysokih Temp.* **19** 22–7 (in Russian)
[20] Kossyi I A, Kostinsky A Yu, Matveyev A A and Silakov V P 1992 *Plasma Sources Sci. Technol.* **1** 207–20
[21] Kondo K and Ikuta N 1990 *J. Phys. Soc. Japan* **59** 3203–16
[22] Person J S and Ham D O 1988 *Radiat. Phys. Chem.* **31** 1–8